Influence of initial oxygen coverage and magnetic moment on the NO decomposition on rhodium (111)

Oliver R. Inderwildi[a] and Dirk Lebiedz
Interdisciplinary Centre for Scientific Computing of the University of Heidelberg, Im Neuenheimer Feld 368, 69120 Heidelberg, Germany

Olaf Deutschmann
Institute of Chemical Technology and Polymer Chemistry, University of Karlsruhe, Engesserstrasse 20, 76131 Karlsruhe, Germany

Jürgen Warnatz
Interdisciplinary Centre for Scientific Computing of the University of Heidelberg, Im Neuenheimer Feld 368, 69120 Heidelberg, Germany

(Received 2 November 2004; accepted 1 February 2005; published online 15 April 2005)

In this study, density functional theory calculations were performed to investigate the influence of oxygen preoccupation on the nitrogen oxide decomposition on rhodium. Besides gauging the coverage dependence of the adsorption energy of NO on the (111) rhodium facet, the influence of the initial oxygen coverage on the kinetics and thermodynamics of the nitrogen oxide decomposition reaction was also studied. The results are discussed with respect to a novel NO_x decomposition catalyst. Furthermore, the influence of spin effects on the adsorption geometry as well as the adsorption energy is examined. It will be addressed why spin effects only have a minor influence on the behavior of NO on a rhodium surface. © *2005 American Institute of Physics*.
[DOI: 10.1063/1.1878692]

I. INTRODUCTION

Legislations in industrial countries are aiming towards the reduction of green house gas emissions. The main green house gas is carbon dioxide and its main source is combustion, mainly in automotive engines. Therefore, alternative modes of drive that emit less green house gas such as fuel cells, electric, or hybrid motors are being developed. Until those alternative modes of drive become a mainstay, the common combustion engine could be improved by operating it under fuel-lean, oxygen-rich condition. Under oxygen-rich conditions, combustion engines are more fuel efficient and consequently emit less green house gas compared to conventional gasoline engines. The disadvantages of lean-run car engines is increased emission of nitrogen oxides (NO_x) and soot.

Apparently, it is a challenging task to chemically reduce a compound in an oxygen rich environment. Different concepts have meanwhile been developed for NO_x reduction. Many approaches do work for model exhaust gases, but most of these catalytic systems are poisoned as soon as minor amounts of sulfur compounds are present in the exhaust. A promising approach for a sulfur resistant $DeNO_x$ catalyst was suggested by Nakatsuji.[1,2] A rhodium-based zeolithic catalyst operated alternately under short lean (time scale of the order of seconds) and very short rich (time scale of the order of 0.1 s) conditions appeared to be sulfur resistant while highly active towards nitrogen oxide decomposition. The NO_x reduction (short, $DeNO_x$) potential is high while the catalyst does not deteriorate when sulfur-containing compounds are added. Nakatsuji proposed a mechanism for the surface processes involved; which suggests that during the oxygen depleted phase, the rhodium surface is reduced, while in the subsequent oxygen rich phase, the NO_x decomposes over the freshly reduced metal surface. It is known that in the absence of oxygen, NO decomposes over a reduced rhodium surface to initially form N_2.[2] This leaves an oxidized rhodium surface that is inactive with respect to further NO decomposition.[3]

Since we are considering exhaust gases with a minor amount of NO_x in a vast excess of oxygen, this implies that NO must decompose much faster on the surface than oxygen does. However, kinetic investigations indicate the contrary.[4]

Various studies have been dedicated to the adsorption geometry and energy of NO on different facets of rhodium.[5] Furthermore, the dissociation of NO was studied with different experimental methods such as temperature programmed desorption (TPD),[6] molecular beam,[4] and scanning tunnel microscopy (STM).[7] In addition, Loffreda *et al.* studied the decomposition of NO on rhodium and the influence of the surface topology on this reaction by means of density functional theory.[8]

It was found by Xu *et al.* that the kinetics depend on the coverage of the Rh(111) surface and that high oxygen preoccupation inhibits the NO decomposition.[7] However, there is no concrete evidence for this coverage dependency. Since experimental measurements of coverage dependencies of the rate coefficients are difficult to conduct, computational *ab initio* studies are promising alternatives to gain a better understanding.

[a]Electronic mail: oliver.inderwildi@iwr.uni-heidelberg.de

In the present study, the decomposition process was studied by means of density functional theory (DFT) calculations to investigate how the surface coverage, especially oxygen preoccupation, influences the decomposition probability of NO on Rh(111). Thermodynamic and kinetic properties of nitrogen oxide adsorption and decomposition have been studied as a function of the initial oxygen coverage.

DFT *ab initio* calculations are becoming a useful tool for estimating kinetic parameters for detailed surface reaction mechanisms for reasons explained in a foregoing publication.[9] Models based on detailed reaction mechanisms are becoming more popular, owing to their higher accuracy and the permanent acceleration of computer processor speed.

II. METHODS

In the present work the reactions of NO on the surface of Rh(111) have been studied by means of DFT calculations using CASTEP (Cambridge sequential total energy package).[10] The generalized gradient approximation (GGA) as proposed by Perdew and Wang[11] was applied combined with Vanderbilt ultrasoft pseudopotentials.[12] Where necessary, spin effects have been taken into account by using the spin polarized (dependent) GGA functional (GGSA). The plane wave basis set was truncated at a kinetic energy of 300 eV. Computations were performed over a range of k points within the Brillouin zone as generated by the Monkhorst–Pack scheme.[13] The precision of the Monkhorst–Pack scheme was chosen so that the k-point spacing is similar for all investigated unit cells.

The surface was modeled as a rhodium slab with the thickness of three atomic layers. Periodic-boundary conditions extrapolate from a metal cluster to an extended surface. Various publications show that the thickness of three layers is sufficient to generate a model of a transition metal surface, exemplarily we refer to a study by Nørskov and co-workers.[14]

Location and the extent of the elementary cell for the DFT calculations were chosen in a way to obtain the surface coverage desired. A 10 Å vacuum was placed in between the periodic slabs to ensure that the adsorbate and the subsequent slab do not interact. The positions of the metal atoms were fixed in (111) surface configuration, while the positions of the adsorbates were fully mobile.

To determine the adsorption energies ΔE_{ads}, the target surface was geometry optimized with the NO molecule added on the one hand and without the NO molecule on the other hand; the energies of the optimized surfaces were calculated subsequent to the geometry optimization. The geometry of the NO molecule was optimized within a cell similar to the cell of the surface and the energy of this optimized NO crystal E_{NO} was calculated subsequently. Finally the adsorption energies were determined according to

$$\Delta E_{\mathrm{ads}} = E_{\mathrm{slab+O_2}} - (E_{\mathrm{slab}} + E_{\mathrm{NO}}). \tag{1}$$

The structures of the reactants and the products were relaxed prior to calculating activation energies, as well as the reaction heats for the NO dissociation. The transition state of the reaction was determined on the potential energy hypersurface by performing a linear synchronous, combined with a quadratic synchronous transit calculation and conjugate gradient refinements.[15] The total energies for the reactants, the transition state and the products were computed. Heats of reaction were calculated according to

$$\Delta E_{\mathrm{reaction}} = E_{\mathrm{products}} - E_{\mathrm{reactants}} \tag{2}$$

and the activation energy was then calculated according to

$$E_{\mathrm{act}} = E_{\mathrm{transition\ state}} - E_{\mathrm{reactants}}. \tag{3}$$

The magnetic moment of a system is expressed by spin densities in the presented work. Spin densities are calculated according to

$$\rho_{spin}(r) = \rho_{\alpha}(r) - \rho_{\beta}(r), \tag{4}$$

with $\rho_{\alpha}(r)$ and $\rho_{\beta}(r)$ denoting the densities of electrons with α and β spin, respectively, at coordinate r. The total electron density of the supercell is calculated according to

$$\rho_{spin}^{total} = \int \rho_{spin}(r)dr. \tag{5}$$

Furthermore, the local electron density is calculated according to

$$\rho_{spin}^{local} = \int |\rho_{spin}(r)|dr. \tag{6}$$

The local electron spin density is a measure of the spin polarization inside a certain system. To assume that a system is nonspin polarized, both the local and the total spin densities have to be zero.

III. RESULTS AND DISCUSSION

A. Nitrogen oxide on rhodium (111)

A (2×2) unit cell of a Rh(111) surface covered with three NO molecules ($\theta=0.75$) was optimized using DFT-GGA calculations. Low-energy electron diffraction (LEED) studies of a Rh(111) surface covered with 0.75 monolayers NO by Zasada *et al.*,[16] found NO to form an ideal hexagonal overlayer with the two NOs arranged in threefold position (fcc and hcp) and one in on-top position. The results of the DFT optimization of this (2×2)-Rh(111) cell with three NO molecules adsorbed leads to exactly the same surface geometry as found by LEED. The calculated surface geometry is depicted in Fig. 1.

All NO molecules are adsorbed perpendicular to the surface with the nitrogen atom pointing towards the surface. A comparison of distances and bond length between the DFT-GGA geometry optimization and the LEED analysis (see Table I) shows that the calculated values are well within the experimental error limits.

Even though the calculated values lie within the experimental error limits, it seems that the DFT calculations slightly overestimate the real values. To verify if this might be due to neglecting spin effects (NO is an odd electron molecule with a doublet ground state), the calculations have been carried out spin polarized. The spin-polarized DFT-GGSA calculation gave exactly the same distances as the

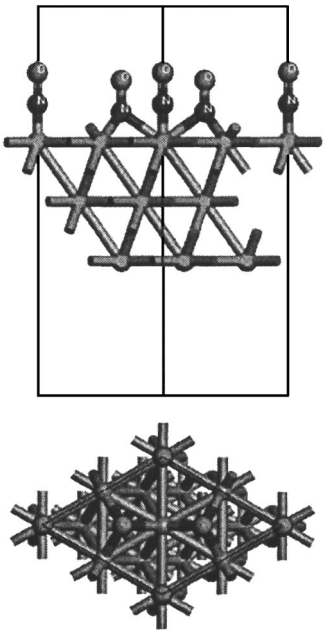

FIG. 1. Front and top view of a (2×2)-3NO on Rh(111).

regular unpolarized (DFT-GGA) calculation, implying, that spin effects do not affect the geometry at all. For direct comparison see Table I. In a study performed by Loffreda *et al.* this is proposed,[8] but no explanation is given. Here this effect was investigated in more detail.

B. Magnetic moment of NO adsorbed on rhodium (111)

In case of free NO, spin effects slightly affect the bonds length (1.23 Å without spin effect, 1.24 Å with spin effects). Therefore, the spin densities for both NO adsorbed on a rhodium (111) surface and NO located remotely (to debar electronic interaction) over a rhodium (111) surface were calculated. These calculations showed that as soon as the NO interacts with the surface, the electronic spin is diluted over the electron gas and hence the effect of the magnetic moment is so minor, that it does not affect the geometry at all.

TABLE I. Comparison between LEED data (Ref. 16) and spin-polarized and unpolarized DFT-GGA-PW91 calculation.

Distance (Å)	LEED	DFT-GGA[a]	DFT-GGSA[b]
	Threefold		
N surface	1.31±0.07 (fcc)	1.36 (fcc)	1.36 (fcc)
	1.29±0.07 (hcp)	1.35 (hcp)	1.35 (hcp)
N–O	1.15±0.07	1.18	1.18
	On-top		
N–O	1.13±0.07	1.18	1.18
Rh–N	1.94±0.08	1.84	1.84
Surface interlayer spacing	2.28±0.04	2.27	2.27

[a]Functional proposed by Perdew and Wang in 1992.
[b]Spin-restricted version of-the functional proposed by Perdew and Wang in 1992.

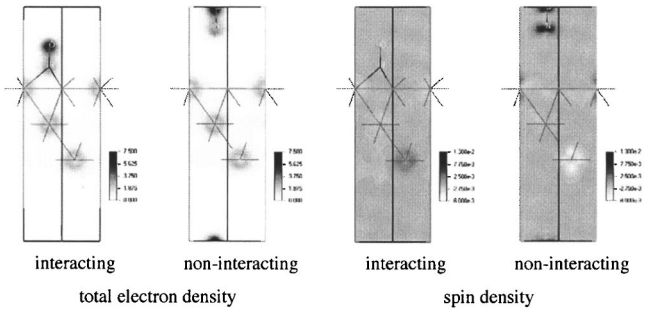

FIG. 2. Spin density plots for nitrogen monoxide adsorbed and NO located remotely over a rhodium (111) surface.

In case of free NO, spin-polarized calculations have calculated ρ_{spin}^{total} and ρ_{spin}^{local} to be 1, predicting the expected doublet state of NO. Upon adsorption of NO on the Rh(111) surface, the calculated total spin density ρ_{spin}^{total} can be considered zero, while the local spin electron density ρ_{spin}^{local} is 0.15. This indicates a weak antiferromagnetic state of the system.

A comparison of the spin density plot of the Rh(111) surface with the interacting and the noninteracting NO shows that in case of the remote NO a high spin density is located on the NO (Fig. 2). The spin density exhibits the symmetry of the antibonding 2π orbital of NO in which the unpaired electron resides. The spin density plot of the interacting analog shows that these high α-spin densities are not present here (no dark areas) while the regions with high β-spin densities (bright areas, third metal layer) vanish as well. This dilution of electronic spin over the electron gas structure leads to same spin density as in the vacuum region above and beneath the metal layer. A general discussion of the origin of adsorbate-induced demagnetization considering NO adsorptions on ferromagnetic nickel as an example is given in Ref. 17.

Energies calculated utilizing the spin restricted and unrestricted GGA functional showed that also the difference in calculated absolute energy is negligible (0.019 eV). The adsorption energies of NO were calculated to be 1.63 eV unaffected by spin effects. Hence, there is no necessity to take spin effect into account in these calculations. The analog plot of the electron density shows that the delocalization of the unpaired electron does not affect the over-all electron density (Fig. 2).

C. Oxygen coverage dependence of the NO adsorption on rhodium (111)

The dependence of the strength of the nitrogen monoxide bonding on the initial oxygen coverage of the rhodium surface has been studied by calculating the heat of adsorption according to 1. It could be shown that the bonding of nitrogen monoxide to the rhodium surface becomes weaker at high oxygen coverage, but remains energetically favorable. The heat of adsorption as a function of the initial surface coverage is depicted in Fig. 3. It indicates that an initial oxygen preoccupation of the rhodium surface thermodynamically inhibits the adsorption of further nitrogen monoxide molecules on the surface. However, compared to the oxygen coverage dependence of the adsorption energy of oxygen

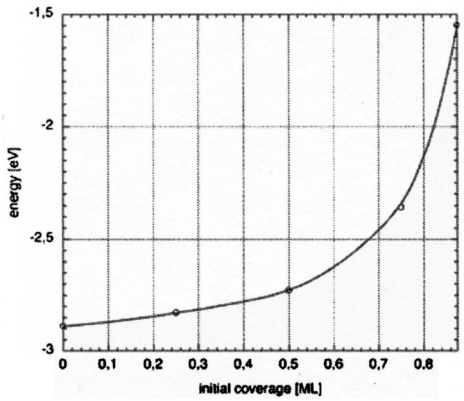

FIG. 3. Heat of adsorption of NO as a function of the oxygen coverage.

which is endothermic at high oxygen coverage (see Ref. 18), the nitrogen monoxide adsorption is still thermodynamically favored over oxygen adsorption at any oxygen preoccupation. This result could support the mechanism proposed by Nakatsuji, because the oxygen coverage would possibly remain at a certain coverage, while NO can still adsorb.

Mulliken charge analysis of the end-on adsorbed NO species with different amounts of oxygen on the surface have been carried out. These analyses showed that the charge transferred from the rhodium surface to the NO molecule decreases with increasing oxygen coverage, see Fig. 4, probably due to the electron withdrawing effect of oxygen. The charges on the nitrogen and oxygen atom decrease stronger above 0.5 ML (monolayer), analogous to the adsorption energy (Fig. 4). These results support the assumption that the origin of this effect is electronic.

D. NO decomposition over rhodium (111) and oxygen influence

The presumption that end-on adsorbed diatomic molecules preferably decompose with the breaking bond coordinated over a single metal atom rather than coordinated over a surface metal-metal bond is well established.[19] Furthermore, it is the common view that end-on adsorbed molecules decompose in a fashion that the generated surface adatoms share the smallest number of surface metal atoms possible

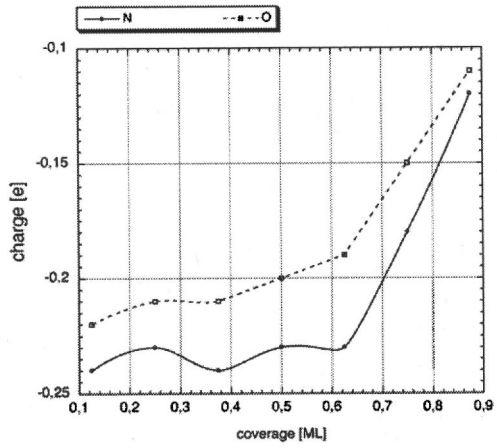

FIG. 4. Mulliken charges as function of the surface coverage.

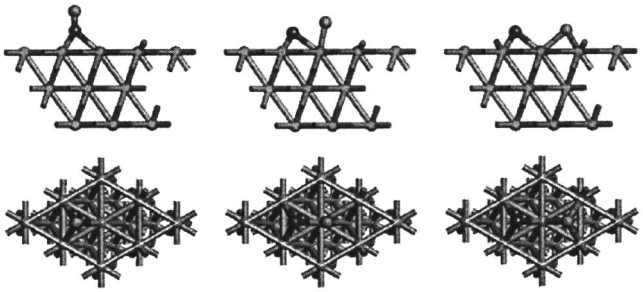

FIG. 5. Adsorbed nitrogen oxide, decomposition transition state, and decomposed nitrogen oxide on (2×2)-rhodium (111).

(principle of least atom sharing).[20] Owing to this, a preferred final conformation of the dissociated molecule was assumed as depicted in Fig. 5, right.

The computed optimal topologies for end-on adsorbed nitrogen oxide as well as its decomposition products are shown in front as well as top view in Fig. 5.

The computed transition state for the decomposition is also depicted and it can be seen that first the nitrogen–oxygen bond has to bend into the direction of the decomposing metal atom. In the transition state the nitrogen–oxygen bond is broken, while both atoms are bonded to the decomposing rhodium surface atom. From the transition state (maximum energy point along the reaction coordinate), the oxygen atom simply "drops" into its preferred adsorption site, meaning that the process is going energetically strictly downhill as expected. The activation energy for this surface reaction was calculated to be 2.24 eV with an energy of reaction of 0.32 eV.

Placing an additional atomic oxygen atom [initial coverage $(\theta_O)=0.25$] on top of the rhodium surface, and recalculating the optimal geometries for starting material as well as the products, a determination of the transition state as described in the Methods section shows that the additional oxygen inhibits further decomposition of NO molecules, even though the decomposition is still sterically unhindered. The activation energy increases to 2.41 eV with an energy of reaction of 0.46 eV.

To investigate this effect in more detail, a surface with a (2×4) elementary cell consisting of eight surface rhodium atoms has been modeled in order to vary the initial oxygen coverage over a broader range. The atomic coordinates of the metal atoms were constrained to conserve the (111) facet, while the adsorbates were assumed to be mobile. Only for high coverage $(\theta\geqslant0.75)$, constraints were imposed on the adsorbates, so that a vacant surface site adjacent to the nitrogen oxide molecule is available to ensure geometrically unhindered decomposition. The geometries for the nitrogen oxide molecule as well as its decomposition products have been calculated for different oxygen coverage. The transition state of the reaction of the molecule to its decomposition products was determined for different initial oxygen coverage. As an example, the transition state of the nitrogen oxide decomposition at an initial oxygen coverage of $\theta_{O,INIT}=0.5$ is shown in Fig. 6, the geometries of all transition state structures are

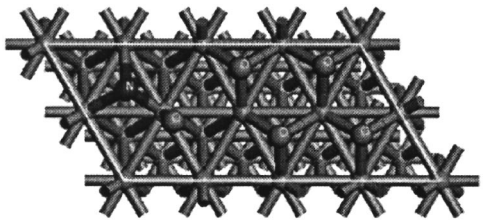

FIG. 6. The transition state of the NO decomposition at an initial oxygen coverage of 0.5 ML.

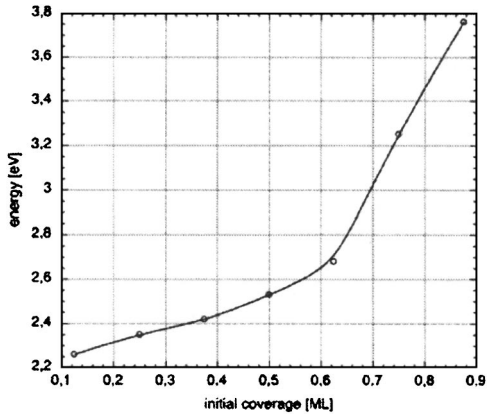

FIG. 7. Activation energy of the NO decomposition as a function of the initial surface coverage.

listed in Table II. The activation energies as well as the reaction enthalpy have been calculated according to Eqs. (2) and (3).

It is shown that for increasing oxygen coverage, the activation energy of the nitrogen oxide decomposition increases (Fig. 7), while the reaction gets more endothermic (Fig. 8). For surface coverages below an initial oxygen coverage of 0.5 ML, the activation energy increases linearly, while it increases almost exponentially above $\theta_O = 0.5$. The calculated over-all reaction [reaction energy gas-phase NO to N and O coadsorbed on Rh(111)] energy of 2.47 eV at 0.25 ML is in close agreement with the value calculated by Loffreda *et al.* (2.5 eV).[8] However, the endothermicity of the dissociation step is clearly in contrast to calculations carried out before.[14] Recalculating the optimal adsorption geometries and the corresponding energies for NO and its dissociation products on a (2×2) elementary cell with the uppermost metal layer allowed to relax, lead as well to an endothermicity of the reaction. An analog study utilizing the spin-restricted functional also calculated the reaction to be endothermic.

This inhibition might be due to the electron withdrawing effect of the adsorbed oxygen. The electronegative oxygen withdraws electrons from the metal surface and hence lowers the backdonation effect of the metal into the antibonding π orbital of the end-on adsorbed nitrogen monoxide. This effect is hindered when oxygen withdraws electrons from the metal atom. The weaker backdonation effect can also be observed in the N–O bond length of the adsorbed NO, it decreases from 1.23 Å ($\theta = 0.125$) to 1.19 Å ($\theta = 1$), indicating a higher bond order of the adsorbed molecule. To verify if electronic effects are also responsible for the increase in activation energy (destabilization of the transition state), Mulliken charge analysis was carried out for the calculated transition states. In Fig. 10, the Mulliken charges are presented as a function of the initial surface coverage. It can be seen that the amount of electronic charge transferred to the transition state structure decreases with increasing surface coverage. This indicates a destabilization of the transition state, which would explain the increase of the activation energy observed.

Furthermore, the heat of formation of the atomic nitrogen and oxygen species decreases with increasing initial coverage. This observation suggests that the capability of rhodium to decompose nitrogen oxide in a vast excess of oxygen is not due to an acceleration by oxygen adsorbed prior to NO decomposition.

IV. CONCLUSIONS

DFT-GGA structure optimizations carried out in this study are able to predict the geometry of adsorbants on Rh(111) accurately. These *ab initio* calculations support the assumption that spin effects do not affect the optimal geometry and energy of NO adsorbed on rhodium (111). Spin-unrestricted calculations show that upon adsorption, NO loses its spin density while it induces a negligible magnetic moment onto the rhodium (111) surface. Hence, further calculations could be carried out with a spin-unrestricted GGA functional, leading to a significant acceleration, especially for the calculations of potential energy hypersurfaces.

TABLE II. Exact geometries of the different transition state structures. ε denotes the angle by which the atoms are tilted out of the surface normal plane, positive angle denotes tilting towards Rh^2 and Rh^5, negative angle towards Rh^1 and Rh^4, α denotes the angle between nitrogen, Rh^3, and oxygen. For atom numbering please see Fig. 9.

	d_{N-Rh} (Å)			N	d_{O-Rh} (Å)			O		N–O
θ_{init}	Rh^1	Rh^2	Rh^3	ε (°)	Rh^3	Rh^4	Rh^5	ε (°)	d_{N-O} (Å)	α (°)
0.125	1.98	2.11	1.99	2.90	2.00	2.99	3.16	5.70	1.99	59.9
0.250	2.01	1.99	2.01	−2.30	1.96	3.03	2.98	−1.60	2.06	62.4
0.375	2.01	1.97	2.02	0.77	2.42	3.55	3.45	2.80	2.11	55.9
0.500	2.07	1.95	2.03	1.10	2.42	3.55	3.45	−3.30	2.12	56.0
0.625	1.98	2.02	1.92	0.80	1.95	3.06	2.95	−3.50	2.03	63.4
0.750	1.90	2.04	1.98	2.90	1.96	2.99	3.20	7.30	2.03	59.8
0.875	2.03	2.09	1.94	1.40	1.97	3.08	2.96	−3.50	1.98	61.0

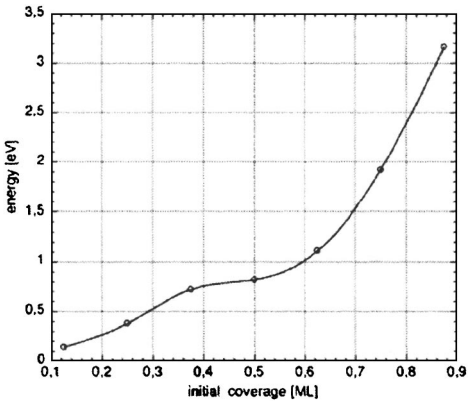

FIG. 8. Coverage dependence of the reaction energies of the NO decomposition.

These spin-unrestricted calculations show that initial oxygen coverage of the rhodium (111) surface weakens the bonding of nitrogen oxide to the rhodium surface. This surmises that with increasing oxygen coverage the adsorption probability of NO decreases, because it gets thermodynamically more unfavorable. However, the thermodynamic inhibition of the oxygen adsorption is more distinct.[18]

Oxygen preoccupation on a rhodium surface abates the ability of rhodium to decompose nitrogen oxide. Since the decomposition process is sterically unhindered (an unoccupied surface site next to the adsorbed oxygen molecule is kept vacant), this increase in activation energy must be due to the electron withdrawing effect of the oxygen. The heat of formation of the atomic species is slightly endothermic (0.15 eV) when NO decomposes on a rhodium (111) surface without oxygen preoccupation (corresponding to 0.125 ML). However, with increasing oxygen preoccupation the reaction gets even more endothermic. These results are in contrast to previous calculations that calculate the decomposition to be exothermic.[14]

Comparing the thermochemistry of desorption and decomposition shows that energetically the decomposition is favored up to 0.75 ML, Fig. 11.

Root *et al.* observed that from 0.3 ML pure NO coverage, not all NO decomposes but desorbs during heating.[6]

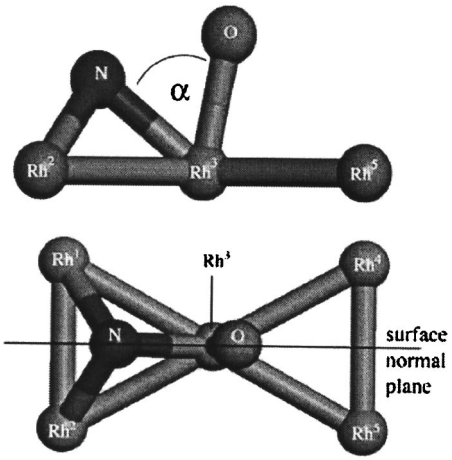

FIG. 9. Example transition state with atom numbering, surface normal plane, and nitrogen–rhodium–oxygen angle α.

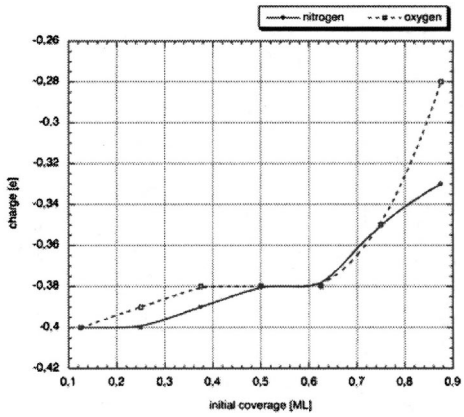

FIG. 10. Mulliken charges of the transition state of the NO decomposition as function of the initial surface coverage.

Considering that owing the decomposition, the surface coverage increases, this is well in agreement with the results found here.

The overall conclusions drawn from this study do not support the surface mechanism proposed by Nakasuji and co-workers.[2] The decrease in NO decomposition activity of the rhodium surface with increasing oxygen coverage points towards a stagnation. The activation energy for the NO decomposition is higher than the activation energy of the oxygen dissociation (see Ref. 9) at any initial oxygen preoccupation and hence, the oxygen dissociation will be more likely at any oxygen preoccupation, see Fig. 12. Although oxygen can decompose in more than one way on Rh(111), e.g., direct dissociative decomposition, the activation barrier for this process will be even lower than that of the end-on O_2.

ACKNOWLEDGMENTS

The presented work was partially supported by German Federal Ministry of Education and Research via the ConNeCat network and by the German Research Foundation via the collaborative research center "Reactive Flows, Diffusion, and Transport." The authors would like to thank the members of the ConNeCat-consortium "Automotive Exhaust Gas Aftertreatment" for advice and guidance. Dr. W.G.

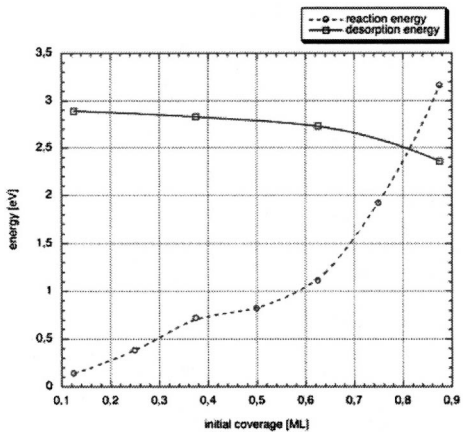

FIG. 11. Thermochemistry of NO desorption and decomposition.

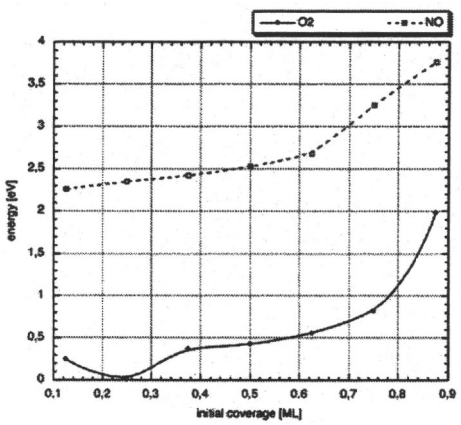

FIG. 12. Activation energies of the oxygen and nitrogen monoxide decomposition as function of the initial coverage.

Bessler and Ravindra Aglave (M.Sc.) (both IWR, University of Heidelberg) are gratefully acknowledged for fruitful discussions.

[1]T. Nakatsuji and V. Komppa, Catal. Today **75**, 407 (2002).
[2]T. Nakatsuji and V. Komppa, Appl. Catal., B **30**, 209 (2001).
[3]K. Almusaiteer, R. Krishnamurthy, and S. S. C. Chuang, Catal. Today **55**, 291 (2000).
[4]C. S. Gopinath and F. Zaera, J. Catal. **200**, 270 (2001).
[5]D. G. Castner, B. A. Sexton, and G. A. Somorjai, Surf. Sci. **71**, 519 (1978); D. G. Castner and G. A. Somorjai, *ibid.* **83**, 60 (1979); F. Garin, Appl. Catal., A **222**, 183 (2003); C.-T. Kao, G. S. Blackman, M. A. v. Hove, and G. A. Somorjai, Surf. Sci. **224**, 77 (1989).
[6]T. W. Root, L. D. Schmidt, and G. B. Fisher, Surf. Sci. Lett. **134**, A410 (1983).
[7]H. Xu and K. Y. S. Ng, Surf. Sci. **365**, 779 (1996).
[8]D. Loffreda, D. Simon, and P. Sautet, J. Catal. **213**, 211 (2003).
[9]O. R. Inderwildi, D. Lebiedz, O. Deutschmann, and J. Warnatz, J. Chem. Phys. **122**, 034710 (2005).
[10]M. D. Segall, P. L. D. Lindan, M. J. Probert, C. J. Pickard, P. J. Hasnip, S. J. Clark, and M. C. Payne, J. Phys.: Condens. Matter **14**, 2717 (2002).
[11]J. P. Perdew, J. A. Chevary, S. H. Vosko, K. A. Jackson, M. R. Pederson, and C. Fiolhais, Phys. Rev. B **46**, 6671 (1992).
[12]D. Vanderbilt, Phys. Rev. B **41**, 7892 (1990).
[13]H. J. Monkhorst and J. D. Pack, Phys. Rev. B **13**, 5188 (1976).
[14]M. Mavrikakis, J. Rempel, J. Greeley, L. B. Hansen, and J. K. Nørskov, J. Chem. Phys. **117**, 6737 (2002).
[15]N. Govind, M. Petersen, G. Fitzgerald, D. King-Smith, and J. Andzelm, Comput. Mater. Sci. **28**, 250 (2003).
[16]I. Zasada, M. A. V. Hove, and G. A. Somorjai, Surf. Sci. Lett. **418**, L89 (1998).
[17]S. J. Jenkins, Q. Ge, and D. A. King, Phys. Rev. B **64**, 012413 (2001).
[18]O. R. Inderwildi, D. Lebiedz, O. Deutschmann, and J. Warnatz, J. Chem. Phys. **122**, 034710 (2005).
[19]R. A. v. Santen and M. Neurock, Catal. Rev. - Sci. Eng. **37**, 557 (1995).
[20]R. A. v. Santen, M. C. Zonnevylle, and A. P. J. Jansen, Philos. Trans. R. Soc. London, Ser. A **341**, 269 (1992).